communications physics

ARTICLE

https://doi.org/10.1038/s42005-021-00709-x OPEN

Particle-hole symmetry and the reentrant integer quantum Hall Wigner solid

Vidhi Shingla[1,3], Sean A. Myers[1,3], Loren N. Pfeiffer[2], Kirk W. Baldwin[2] & Gábor A. Csáthy[1✉]

The interplay of strong Coulomb interactions and of topology is currently under intense scrutiny in various condensed matter and atomic systems. One example of this interplay is the phase competition of fractional quantum Hall states and the Wigner solid in the two-dimensional electron gas. Here we report a Wigner solid at $\nu = 1.79$ and its melting due to fractional correlations occurring at $\nu = 9/5$. This Wigner solid, that we call the reentrant integer quantum Hall Wigner solid, develops in a range of Landau level filling factors that is related by particle-hole symmetry to the so called reentrant Wigner solid. We thus find that the Wigner solid in the GaAs/AlGaAs system straddles the partial filling factor 1/5 not only at the lowest filling factors, but also near $\nu = 9/5$. Our results highlight the particle-hole symmetry as a fundamental symmetry of the extended family of Wigner solids and paint a complex picture of the competition of the Wigner solid with fractional quantum Hall states.

[1] Department of Physics and Astronomy, Purdue University, West Lafayette, IN, USA. [2] Department of Electrical Engineering, Princeton University, Princeton, NJ, USA. [3] These authors contributed equally: Vidhi Shingla, Sean A. Myers. ✉email: gcsathy@purdue.edu

One of the most stunning effects of strong interactions is the formation of interaction-driven topological states, such as the fractional quantum Hall states (FQHSs) developing in clean two-dimensional electron gases (2DEGs)[1]. A fundamental symmetry that governs the fractional quantum Hall regime is the particle–hole symmetry[2–4]. While particle–hole symmetry is commonly applied to the physics of the 2DEG, highly non-trivial aspects of this symmetry were not appreciated until recently. Indeed, particle–hole symmetry near the Fermi sea of composite fermions was found to have deep implications for the understanding of this Fermi sea[5], explicit particle–hole symmetry was only recently demonstrated for transport and FQHS energy gaps[6], and the examination of particle–hole symmetry for the even denominator FQHSs broadened concepts of topological order significantly[7–11].

Besides generating novel topological states, strong interactions in clean 2DEGs also order charge carriers into electron solids[12,13]. Due to the flat nature of energy bands at high magnetic fields, one way for electrons to minimize their Coulomb energy is through ordering into a triangular lattice called the Wigner solid (WS). The insulating phase at Landau level filling factors $\nu < 1/5$ forming in the 2DEG in GaAs/AlGaAs heterostructures has long been interpreted as a WS, often called the high-field WS (HFWS)[14–18]. Results from a variety of experiments, such as nonlinear transport[19–21], noise[22], dielectric constant measurement[23], microwave spectroscopy[24–26], composite fermion commensuration oscillations[27], and screening measurements[28], have strengthened this interpretation. Since the HFWS and the terminal FQHS at $\nu = 1/5$ form in the same range of magnetic fields, these two phases often display a competition that determines the structure of the phase diagram[14–16,29,30].

Wigner crystallization in the 2DEG is energetically favored not only at $\nu < 1/5$ but also at other values of the filling factor. These WSs bear different names. For example, the WS that develops in the $1/5 < \nu < 2/9$ range of filling factors is called the reentrant WS (RWS)[16]. Furthermore, the WS referred to as integer quantum Hall WS (IQHWS) forms in the flanks of integer quantum Hall states (IQHS)[31–39]. IQHWSs have relatively large quasiparticle densities at which the Anderson insulator in the bulk of the 2DEG reorganizes itself into a WS once the Coulomb energy overtakes disorder effects. IQHWSs were discovered by the detection of their pinning modes[31–33], but were also observed in nuclear magnetic resonance[34], compressibility[35], surface acoustic wave propagation[36], tunneling measurements[37], and recent transport measurements[38,39]. While the above WSs were discovered in GaA/AlGaAs hosts, recent progress with the quality of other host materials yielded similar physics. For example, Wigner crystallization has recently been observed in the ZnO/ZnMgO system[40,41], graphene[42], and in AlAs quantum wells[43].

Here, we report the observation of an electron solid near the filling factor $\nu = 1.79$ in clean 2DEGs confined to GaAs/AlGaAs hosts. The transport signatures of this phase, a vanishing magnetoresistance accompanied by a Hall resistance that is quantized to $R_{xy} = h/2e^2$, allow us to infer that this electron solid is a WS. The WS at $\nu = 1.79$ develops near the IQHWS, but it is distinct from the latter. We, therefore, term this WS the reentrant IQHWS (RIQHWS). We find that the RIQHWS is related by particle–hole symmetry to the RWS that develops at high magnetic fields. This means that the elementary building blocks of the RIQHWS are quasiholes, rather than quasielectrons, and we establish that particle–hole symmetry is a fundamental symmetry that extends over the larger family of WSs. In addition, our observations reveal that the phase competition of the RIQHWS and an FQHS that forms nearby is a generic property for 2DEGs with strong interactions, which has an imprint on the wider phase diagram.

Results and discussion

Magnetotransport of our Sample 1 measured at $T = 12$ mK reveals a rich structure exhibiting various known ground states of the 2DEG. In Fig. 1 we identify a few prominent examples, such as the $\nu = 2$, 3, and 4 IQHS, several FQHSs, including a rich structure in the $N = 1$ Landau level[44–46]. In addition, the $\nu > 4$ range is dominated by various electronic stripe and bubble phases[47–51]. We focus our attention on the range of filling factors delimited by the $\nu = 2$ IQHS and the $\nu = 5/3$ FQHS, i.e., the region near $B = 7.25$ T. In this region in Fig. 1, we observe structures in the longitudinal magnetoresistance R_{xx}.

The region $5/3 < \nu < 2$ is shown in greater detail in Fig. 2. In the $T = 300$ mK magnetoresistance R_{xx} trace of Fig. 2, three local minima are signaling the development of FQHSs. One is at $\nu = nh/eB = 12/7$. Here, n is the electron density, B is the magnetic field, e is the electron charge, and h is Planck's constant. A resistance minimum at $\nu = 12/7$ was attributed to an FQHS[52]. In addition, in the $T = 300$ mK R_{xx} trace, there is another so far unreported resistance minimum at a higher filling factor $\nu = 9/5$. Hall resistance measurements at these two filling factors, $\nu = 12/7$ and $\nu = 9/5$, reveal inflections close to $7h/12e^2$ and $5h/9e^2$, respectively. These data are therefore suggestive of developing fractional correlations associated with FQHSs at $\nu = 12/7$ and 9/5. These and other Landau level filling factors of interest are marked in Fig. 2 by dashed vertical lines.

Observation of a collective insulator at $\nu = 1.79$ and its competition with the $\nu = 9/5$ FQHS. Even though at $T = 300$ mK we identified similar behavior at both $\nu = 12/7$ and 9/5, we find that the temperature evolution of the magnetoresistance at these two filling factors is very different. Indeed, as the temperature is

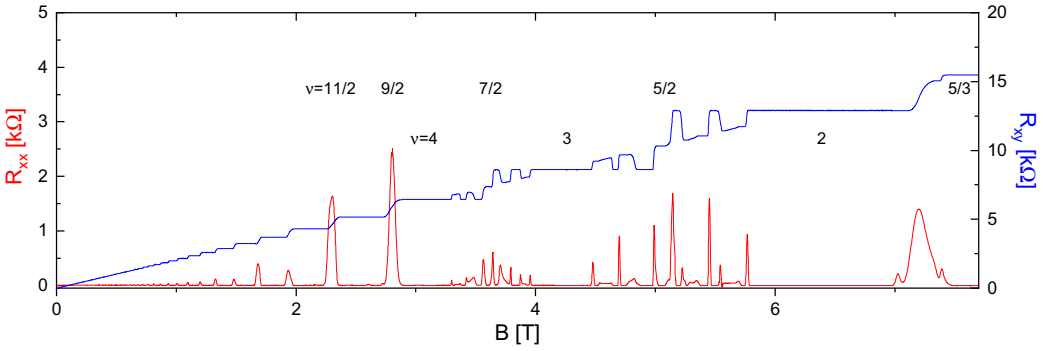

Fig. 1 Magnetoresistance R_{xx} and Hall resistance R_{xy} of Sample 1 over a broad range of magnetic fields B. Traces are obtained at the temperature $T = 12$ mK. Numerical labels indicate notable Landau level filling factors ν. Structures of interest develop near $B = 7.25$ T, in the range of filling factors $5/3 < \nu < 2$.

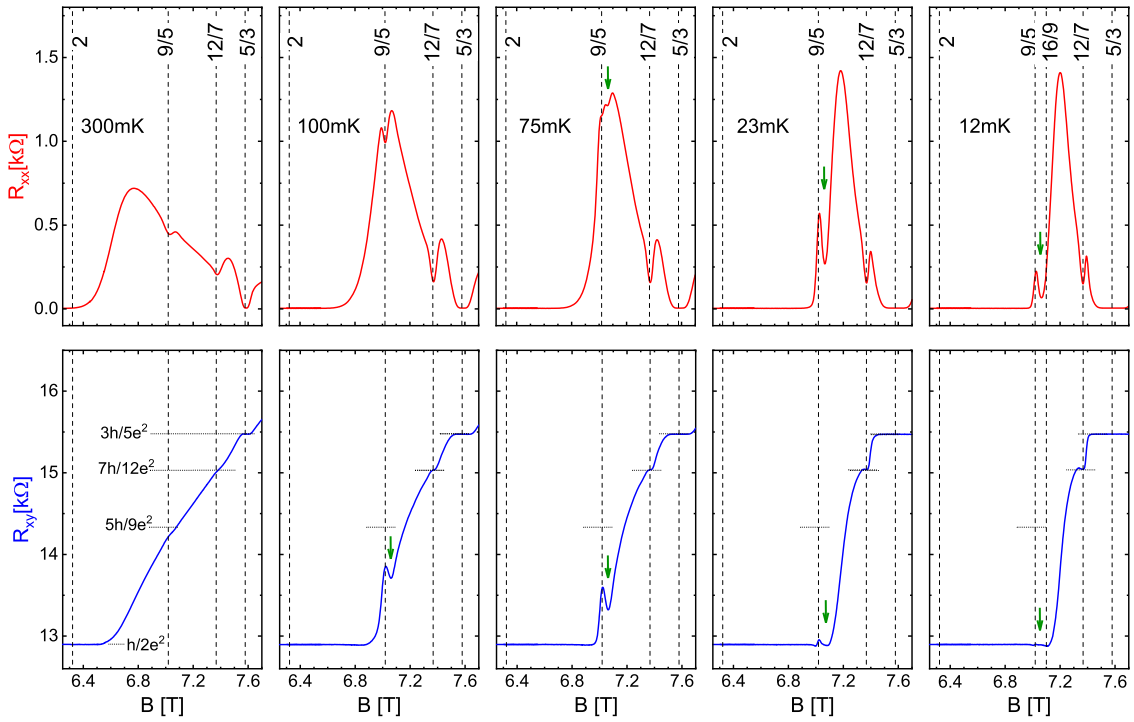

Fig. 2 The dependence on temperature *T* of the magnetoresistance R_{xx} and Hall resistance R_{xy} of Sample 1 in the range of filling factors $5/3 < \nu < 2$. Labels on vertical dashed lines are filling factors ν of interest. The electron solid we refer to as the reentrant integer quantum Hall Wigner solid (RIQHWS) is located between filling factors $\nu = 9/5$ and 16/9 and it is marked by arrows.

lowered from $T = 300$ mK, the inflection in the Hall resistance at $\nu = 12/7$ persists. As shown in Fig. 2, at the lowest temperature of $T = 12$ mK, R_{xx} maintains its local minimum and R_{xy} is quantized to $7h/12e^2$. However, R_{xx} at this filling factor changes very little with temperature. This indicates a weak FQHS at $\nu = 12/7$. In contrast, the behavior near $\nu = 9/5$ is qualitatively different. The local minimum in R_{xx} at $\nu = 9/5$ is still present at $T = 100$ mK, but it rides on a magnetoresistance background that rises with lowering the temperature. Indeed, as seen in Fig. 2, R_{xx} near $\nu = 9/5$ at $T = 100$ mK is approximately doubled as compared to that at $T = 300$ mK. Furthermore, the local minimum in R_{xx} at $\nu = 9/5$ is extremely weak at $T = 75$ mK and it is no longer present at $T < 75$ mK. We conclude that at temperatures $T \geq 75$ mK, our sample exhibits signs of fractional correlations at $\nu = 9/5$. However, at the lowest accessed temperatures, our sample does not support a fractional quantum Hall ground state at $\nu = 9/5$.

An unusual feature of the $T = 75$ mK R_{xx} data is that there is a local minimum in R_{xx}, which, however, is at a distinctively different filling factor than 9/5. This new minimum in R_{xx}, marked by arrows in Fig. 2, develops at $\nu = 1.79$. This filling factor is not a part of the standard sequence of fractional valued filling factors[3]; therefore, the minimum in R_{xx} at $\nu = 1.79$ most certainly cannot be associated with an FQHS. This conclusion is strengthened by our observations of the Hall resistance at $T \leq 75$ mK, which deviates significantly from any possible plateau values expected for an FQHS that may develop near $\nu = 1.79$. Instead, as the temperature is lowered, R_{xx} at $\nu = 1.79$ gradually decreases towards $R_{xx} = 0$ and R_{xy} becomes quantized to $R_{xy} = h/2e^2$. This is seen in the $T = 23$ mK and $T = 12$ mK traces shown in Fig. 2. Such a behavior signals collective localization, i.e., the development of an electron solid[49–51]. In Fig. 2 we marked this electron solid at $\nu = 1.79$ with arrows. Since a similar transport signature is present along a perpendicular crystal direction, this electron solid is isotropic.

Relating the electron solid at $\nu = 1.79$ and the IQHWS. In order to understand the nature of the electron solid forming at $\nu = 1.79$, we recall that complex electron solids called electronic bubble phases form in high Landau levels. Bubble phases are a triangular lattice of electron bubbles, formed of electrons clustered together[47–51]. The clustering of several electrons into a bubble is afforded by the nodal structure of the single electron wavefunction and it is consistent with the most recent experimental observations[53,54]. The electronic wavefunction in the $N = 0$ Landau level does not have any nodes; therefore, among the electronic bubble phases, only the one-electron bubble phase may form, a phase that is identical to the WS[47,48]. Other charge-ordered phases we have to consider are the ones constituted by quasiparticles of FQHSs, such as the WS of composite fermions[55–58]. However, because the Hall resistance is not quantized to a fractional value, in our experiment we have no evidence of the formation of such quasiparticles at $\nu = 1.79$. Since our electron solid forms in the $N = 0$ Landau level, where multi-electron bubble phases are not expected, and since at $\nu = 1.79$ we have no evidence of quasiparticles of FQHSs, we identify the solid at this filling factor with a WS.

As discussed in the "Introduction," WSs termed IQHWSs are known to form in the flanks of integer plateaus[31–39], specifically in the flanks of the $\nu = 2$ IQHS as well[31,34]. IQHWSs form within the range of filling factors $0 < |\nu^*| < 1/5$, albeit the stability range is expected to be temperature and disorder dependent[31–39]. Here, the partial filling factor near $\nu = 2$ is $\nu^* = \nu - 2$. The partial filling factor of the $\nu = 1.79$ WS is $|\nu^*| = 0.21$, which is clearly outside the range of formation of the IQHWS. Hence, the $\nu = 1.79$ WS forms at a larger quasiparticle density than the nearby IQHWS. When a ground state becomes unstable for a small range of parameters and then reappears, it is called a reentrant ground state. We will thus refer to the $\nu = 1.79$ WS as the RIQHWS.

Before further analysis, we check that the filling factor of the formation of the RIQHWS is independent of the experimental

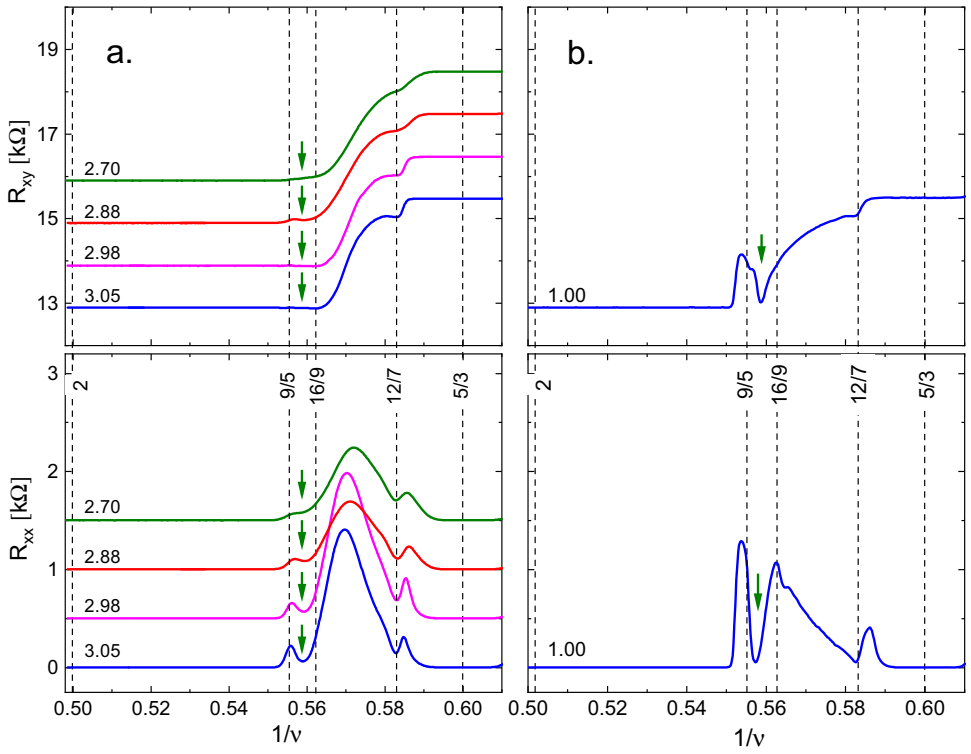

Fig. 3 Reentrant integer quantum Hall Wigner solids in a variable density sample and a sample of fixed density. a Waterfall plots of the magnetoresistance R_{xx} and Hall resistance R_{xy} as plotted against the inverse filling factor $1/\nu$ of Sample 1 as prepared at different electron densities. Measurements were performed at the temperature of $T = 12$ mK. **b** Magnetoresistance R_{xx} and Hall resistance R_{xy} as plotted against the inverse filling factor $1/\nu$ of Sample 2 of a fixed electron density. This density is significantly lower than that of Sample 1. Measurements were performed at the temperature of $T = 5.1$ mK. Labels on traces indicate electron densities n in units of 10^{11} cm^{-2}. Vertical dashed lines mark locations and values of filling factors ν of interest and arrows mark the reentrant integer quantum Hall Wigner solid (RIQHWS). With the exception of traces at the highest density, traces for Sample 1 are shifted vertically upward for clarity.

parameters we control. We have already shown that the RIQHWS develops at a T-independent B-field, and therefore a T-independent filling factor. In addition, the RIQHWS also develops at a density-independent filling factor. In Fig. 3 we show the evolution of magnetoresistance with the density. Here, we demonstrate that as the density of Sample 1 is lowered from 3.05×10^{11} to 2.70×10^{11} cm^{-2}, the RIQHWS develops at the same ν. Furthermore, the RIQHWS also develops at the same filling factor in Sample 2 of a much reduced density 1.0×10^{11} cm^{-2}. We think that the development of the RIQHWS in Sample 2 is aided by its unusually high mobility and a wider width of the quantum well. The temperature and density independence of magnetoresistance features associated with the RIQHWS establishes the RIQHWS as a genuine ground state of the 2DEG over a wide range of electron densities.

Relating the electron solid at $\nu = 1.79$ and other WSs. Further insight on the nature of the RIQHWS may be gained from considering particle–hole symmetry, a fundamental symmetry of the Hamiltonian of electrons in two dimensions that connects ground states at different filling factors sharing the same absolute value of the partial filling factor $|\nu^*|$[2–4]. The $2 - 1/5 < \nu < 2$ range of stability of the IQHWS and the range of stability $\nu < 1/5$ of the HFWS share the same range of partial filling factors $|\nu^*| < 1/5$. It is said that the IQHWS and the HFWS are linked by the $\nu \leftrightarrow 2 - \nu$ particle–hole symmetry, or HFWS $\leftrightarrow$ IQHWS. We notice that the RIQHWS and the RWS are also linked by particle–hole symmetry, i.e., RWS $\leftrightarrow$ RIQHWS. Indeed, the RIQHWS forms in the range $9/5 = 2 - 1/5 < \nu < 2 - 2/9 = 16/9$. The range of filling factors of $2 - 1/5 < \nu < 2 - 2/9$, the RIQHWS corresponds to partial fillings $1/5 < |\nu^*| < 2/9$ and it is indeed related by the same $\nu \leftrightarrow 2 - \nu$ symmetry to the $1/5 < \nu < 2/9$ range of the RWS[16]. This means that the RWS is a WS of electrons, whereas the RIQHWS is a WS of hole quasiparticles and both of these solids form in the same range of partial filling factors. The stability ranges of the various WSs, including that of the RIQHWS, and their symmetries are on display in Fig. 4. All WSs marked in this figure straddle the partial filling factor $|\nu^*| = 1/5$ and obey particle–hole symmetry. As a consequence, we found that the RIQHWS, the newest member of the WS family, together with other WSs, admit particle–hole symmetry as a fundamental property.

Our results find a natural explanation if one assumes that the IQHWS and the RIQHWS are part of the same monolithic WS phase. This monolithic WS phase straddles the filling factor $\nu = 9/5$, i.e., it is present on both sides of $\nu = 9/5$. The resistive peak in R_{xx} seen at $\nu = 9/5$ in Fig. 3 and also in Fig. 2 at the four lowest temperatures is then due to melting of this WS due to remnant fractional correlations at this filling factor. The observed magnetotransport thus indicates a competition of two strongly correlated ground states: the WS and the $\nu = 9/5$ FQHS. Invoking such remnant correlations at $\nu = 9/5$ is not unreasonable since their effect may be observed in Fig. 2 as an incipient FQHS at $75 \le T \le 300$ mK. These fractional correlations in our sample are, however, not strong enough to allow the development of a fully quantized fractional quantum Hall ground state at $\nu = 9/5$. Indeed, according to data plotted in Fig. 3, $R_{xx}(\nu = 9/5) \neq 0$ and $R_{xy}(\nu = 9/5) \neq 5h/9e^2$ for both samples. R_{xy} at $\nu = 9/5$ has a shoulder in Sample 2, but $R_{xy}(\nu = 9/5)$ is 3.4% less than $5h/9e^2$. A similar situation was encountered in early experiments on low

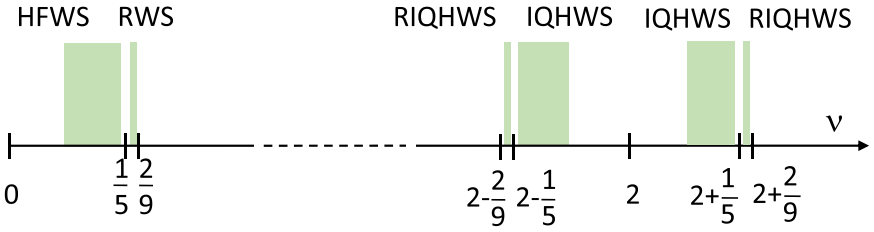

Fig. 4 Schematic diagram of the stability regions of the various Wigner solids in GaAs/AlGaAs system. The Wigner solid we report on is the reentrant integer quantum Hall Wigner solid (RIQHWS), seen between the filling factors $\nu = 2 - 1/5$ and $2 - 2/9$. The high-field Wigner solid (HFWS) and integer quantum Hall Wigner solid (IQHWS) are related by particle-hole symmetry. Similarly, the reentrant Wigner solid (RWS) and the reentrant integer quantum Hall Wigner solid (RIQHWS) are also related by particle-hole symmetry.

mobility 2DEGs in which insulating behavior was seen on both sides of $\nu = 1/5$, i.e. in which both the HFWS and the RWS were present, but an FQHS at $\nu = 1/5$ between these WSs did not fully develop[14,15]. Therefore our results show that the competition of WSs and the FQHS that they straddle is a generic feature of phase competition in regions where WSs form.

The WSs discussed so far form in the $N = 0$ orbital Landau level, i.e., in the $0 < \nu < 2$ range. We suggest that the above properties of the WS may be further extended even into the $N = 1$ Landau level. The IQHWS was known within the $2 < \nu < 2 + 1/5$ range[31,34], and in an earlier publication, a WS was found at $\nu = 2.21$, clearly confined to the $2 + 1/5 < \nu < 2 + 2/9$ range[59,60]. For this WS $1/5 < |\nu^*| < 2/9$ and based on our arguments put forth earlier, we identify this WS at $\nu = 2.21$ with the RIQHWS. Furthermore, there is a monolithic WS phase in this region that straddles both sides of $\nu = 2 + 1/5$ FQHS and which is melted by the fractional correlations of this FQHS. This RIQHWS is related by particle–hole symmetry to both the RIQHWS at $\nu = 1.79$ and to the RWS, and it is included in the diagram shown in Fig. 4. We note that in Sample 1 this WS at $\nu = 2.21$ did not develop. The reason for this is unknown, but differences in density, mobility, different measurement temperatures, and a different background impurity profile due to the different growth chambers are possible culprits.

Most recently, electron solids in the $N = 0$ Landau level were also reported close to $\nu = 1$[38,39]. Some of these are in the range of filling factors associated with the IQHWS. Others, such as the ones forming at $\nu = 0.78$ in a 42, 44[38], and a 65 nm quantum well sample[39] develop at partial filling factor $|\nu^*| = 0.22$. These electron solids were first interpreted as WSs[38], and then later as exotic solids formed of composite fermions[39]. The partial filling factor of these electron solids is stunningly close to that of the RIQHWS we found. One possibility is thus that these WSs are identical to the RIQHWS, particle–hole symmetric counterparts of the RWS. Nonetheless, the nature of these electron solids remains to be determined; softening of the short-range part of the effective electron–electron interaction that occurs in samples with wide quantum wells is known to tune the formation of electron solids and may stabilize various types of electronic solids.

A shared feature of the WSs in our electron samples is that they straddle the partial filling factor $|\nu^*| = 1/5$. In other systems, however, WSs may straddle other partial filling factors. For example, in two-dimensional hole gases (2DHGs), the WS straddles $\nu^* = \nu = 1/3$[61–63]. This difference between 2DEGs and 2DHGs is attributed to the significantly larger ratio of the Coulomb interaction and Fermi energies in the latter[61,62]. Furthermore, the WS in 2DEGs in very narrow quantum wells straddles $\nu = 1/3$[64] and WSs form in samples with added short-range disorder near $|\nu^*| = 1/3$[65]. In yet other systems, phases associated with the WS may straddle more than just one FQHS. This is the case of a 2DEG realized in the ZnO/MgZnO system in which the WS was found to straddle several FQHSs[41]. These experiments suggest that disorder influences the range of stability of the WS and highlight that there is still much to be understood about disorder effects.

Conclusions

We reported complex features of the magnetoresistance at $\nu = 1.79$ in the $N = 0$ Landau level of two high-mobility 2DEGs confined to GaAs/AlGaAs. In contrast to similar transport features in high $N \geq 2$ Landau levels, the ground state at $\nu = 1.79$ is associated with a WS. Because of its proximity to the IQHWS, we named this WS the RIQHWS. Based on the stability region in the filling factor space, the RIQHWS and another RIQHWS reported at $\nu = 2.21$ in the $N = 1$ Landau level[59,60] can both be understood as the particle–hole symmetric counterparts of the RWS. Our results indicate that WSs in the GaAs/AlGaAs system straddle the partial filling factor $|\nu^*| = 1/5$, that particle–hole symmetry of the WS is more pervasive than previously thought, and that this symmetry leads to competing WSs and FQHSs in unexpected parts of the phase diagram.

Methods

Samples. Sample 1 is a 2DEG confined to a 30 nm GaAs quantum well that is part of a GaAs/AlGaAs heterostructure. The density of this sample is $n = 3.05 \times 10^{11}$ cm^{-2} and low- temperature mobility is $\mu = 3.2 \times 10^7$ cm^2/Vs. The 2DEG is doped in a superlattice. The sample state was prepared with illumination with a red light-emitting diode at 10 K according to a procedure described in ref. [66].

Sample 2 is also a 2DEG confined to a GaAs/AlGaAs heterostructure, but differs in several aspects from Sample 1. It belongs to the most recent generation of high-mobility samples[67]. Its density is significantly less than that of Sample 1, $n = 1.0 \times 10^{11}$ cm^{-2}, and its mobility is $\mu = 3.5 \times 10^7$ cm^2/Vs. The width of the confining quantum well in Sample 2 is 49 nm, significantly larger than that of Sample 1. We note that since the mobility of Sample 2 is very large, the second electric subband in this sample is not populated.

Experimental techniques. Magnetotransport measurements were performed in a van der Pauw sample geometry using the standard lock-in technique. The square-shaped samples have eight indium ohmic contacts placed in the corners and the middle of the sides. The excitation current used was 3 nA. Sample 1 was mounted in a vacuum on the copper tail of our dilution refrigerator, reaching the lowest estimated temperature of $T = 12$ mK. In contrast, Sample 2 was mounted inside a He-3 immersion cell, with the lowest bath temperature reached in our current measurement being $T = 5.1$ mK[68]. In this setup, the electronic temperature follows closely that of the bath[68]. For temperature measurements, a carbon thermometer was used[69], which below 100 mK was calibrated against a He-3 quartz tuning fork viscometer[68].

The density of Sample 1 was reduced from its maximum value by using a cold illumination technique described in ref. [66]. As a result of this process, sample parameters changed from 3.05×10^{11} cm^{-2} and $\mu = 3.2 \times 10^7$ cm^2/Vs to 2.70×10^{11} cm^{-2} and $\mu = 1.3 \times 10^7$ cm^2/Vs. We passed bursts of current of 1 μA through a red light-emitting diode for a duration of about 5 s, while the sample was kept near the base temperature of the refrigerator and at $B = 0$. For the illumination procedure to work, it is critical that the light beam covers the area of the sample uniformly. To achieve this, the diode faces the sample, it is centered onto the sample, and it is mounted at a distance of 1.5 cm from the sample.

Data availability

The data that support the findings of this study are available from the corresponding author upon request.

Received: 22 June 2021; Accepted: 23 August 2021;
Published online: 10 September 2021

References

1. Tsui, D. C., Stormer, H. L. & Gossard, A. C. Two-dimensional magnetotransport in the extreme quantum limit. *Phys. Rev. Lett.* **48**, 1559–1562 (1982).
2. Girvin, S. M. Particle-hole symmetry in the anomalous quantum Hall effect. *Phys. Rev. B* **29**, 6012–6014 (1984).
3. Jain, J. K. Composite-fermion approach for the fractional quantum Hall effect. *Phys. Rev. Lett.* **63**, 199–202 (1989).
4. Balram, A. C. & Jain, J. K. Nature of composite fermions and the role of particle-hole symmetry: a microscopic account. *Phys. Rev. B* **93**, 235152 (2016).
5. Hossain, M. S. et al. Precise experimental test of the Luttinger theorem and particle-hole symmetry for a strongly correlated fermionic system. *Phys. Rev. Lett.* **125**, 046601 (2020).
6. Pan, W. et al. Particle-hole symmetry and the fractional quantum Hall effect in the lowest Landau level. *Phys. Rev. Lett.* **124**, 156801 (2020).
7. Levin, M., Halperin, B. I. & Rosenow, B. Particle-hole symmetry and the Pfaffian state. *Phys. Rev. Lett.* **99**, 236806 (2007).
8. Lee, S.-S., Ryu, S., Nayak, C. & Fisher, M. P. A. Particle-hole symmetry and the $\nu = 5/2$ quantum Hall state. *Phys. Rev. Lett.* **99**, 236807 (2007).
9. Son, D. T. Is the composite fermion a Dirac particle? *Phys. Rev. X* **5**, 031027 (2015).
10. Zucker, P. T. & Feldman, D. E. Stabilization of the particle-hole Pfaffian order by Landau-level mixing and impurities that break particle-hole symmetry. *Phys. Rev. Lett.* **117**, 096802 (2016).
11. Wan, X. & Yang, K. Striped quantum Hall state in a half-filled Landau level. *Phys. Rev. B* **93**, 201303 (2016).
12. Wigner, E. On the interaction of electrons in metals. *Phys. Rev.* **46**, 1002–1011 (1934).
13. Lozovik, Y. E. & Yudson, V. I. Feasibility of superfluidity of paired spatially separated electrons and holes; a new superconductivity mechanism. *JETP Lett.* **22**, 11 (1975).
14. Goldman, V. J., Shayegan, M. & Tsui, D. C. Evidence for the fractional quantum Hall state at $\nu = 1/7$. *Phys. Rev. Lett.* **61**, 881–884 (1988).
15. Willett, R. L. et al. Termination of the series of fractional quantum Hall states at small filling factors. *Phys. Rev. B* **38**, 7881–7884 (1988).
16. Jiang, H. W. et al. Quantum liquid versus electron solid around $\nu = 1/5$ Landau-level filling. *Phys. Rev. Lett.* **65**, 633–636 (1990).
17. Paalanen, M. A. et al. Electrical conductivity and Wigner crystallization. *Phys. Rev. B* **45**, 13784–13787 (1992).
18. Pan, W. et al. Transition from an electron solid to the sequence of fractional quantum Hall states at very low Landau level filling factor. *Phys. Rev. Lett.* **88**, 176802 (2002).
19. Goldman, V. J., Santos, M., Shayegan, M. & Cunningham, J. E. Evidence for two-dimensional quantum Wigner crystal. *Phys. Rev. Lett.* **65**, 2189–2192 (1990).
20. Jiang, H. W., Stormer, H. L., Tsui, D. C., Pfeiffer, L. N. & West, K. W. Magnetotransport studies of the insulating phase around $\nu = 1/5$ Landau-level filling. *Phys. Rev. B* **44**, 8107–8114 (1991).
21. Williams, F. I. B. et al. Conduction threshold and pinning frequency of magnetically induced Wigner solid. *Phys. Rev. Lett.* **66**, 3285–3288 (1991).
22. Li, Y. P., Sajoto, T., Engel, L. W., Tsui, D. C. & Shayegan, M. Low-frequency noise in the reentrant insulating phase around the 1/5 fractional quantum Hall liquid. *Phys. Rev. Lett.* **67**, 1630–1633 (1991).
23. Li, Y. P. et al. Observation of a giant dielectric constant in the re-entrant insulating phase of two-dimensional electrons. *Solid State Commun.* **95**, 619–623 (1995).
24. Andrei, E. Y. et al. Observation of a magnetically induced Wigner solid. *Phys. Rev. Lett.* **60**, 2765–2768 (1988).
25. Ye, P. D. et al. Correlation lengths of the Wigner-crystal order in a two-dimensional electron system at high magnetic fields. *Phys. Rev. Lett.* **89**, 176802 (2002).
26. Chen, Y. P. et al. Melting of a 2D quantum electron solid in high magnetic field. *Nat. Phys.* **2**, 452–455 (2006).
27. Deng, H. et al. Commensurability oscillations of composite fermions induced by the periodic potential of a Wigner crystal. *Phys. Rev. Lett.* **117**, 096601 (2016).
28. Deng, H. et al. Probing the melting of a two-dimensional quantum Wigner crystal via its screening efficiency. *Phys. Rev. Lett.* **122**, 116601 (2019).
29. Lam, P. K. & Girvin, S. M. Liquid-solid transition and the fractional quantum-Hall effect. *Phys. Rev. B* **30**, 473–475 (1984).
30. Levesque, D., Weis, J. J. & MacDonald, A. H. Crystallization of the incompressible quantum-fluid state of a two-dimensional electron gas in a strong magnetic field. *Phys. Rev. B* **30**, 1056–1058 (1984).
31. Chen, Y. P. et al. Microwave resonance of the 2D Wigner crystal around integer Landau fillings. *Phys. Rev. Lett.* **91**, 016801 (2003).
32. Lewis, R. M. et al. Evidence of a first-order phase transition between Wigner-crystal and bubble phases of 2D electrons in higher Landau levels. *Phys. Rev. Lett.* **93**, 176808 (2004).
33. Lewis, R. M. et al. Wigner crystallization about $\nu = 3$. *Phys. E* **22**, 104–107 (2004).
34. Tiemann, L., Rhone, T. D., Shibata, N. & Muraki, K. NMR profiling of quantum electron solids in high magnetic fields. *Nat. Phys.* **10**, 648–652 (2014).
35. Zhang, D., Huang, X., Dietsche, W., von Klitzing, K. & Smet, J. H. Signatures for Wigner crystal formation in the chemical potential of a two-dimensional electron system. *Phys. Rev. Lett.* **113**, 076804 (2014).
36. Drichko, I. L. et al. Crossover between localized states and pinned Wigner crystal in high-mobility n-GaAs/AlGaAs heterostructures near filling factor $\nu = 1$. *Phys. Rev. B* **92**, 205313 (2015).
37. Jang, J., Hunt, B. M., Pfeiffer, L. N., West, K. W. & Ashoori, R. C. Sharp tunnelling resonance from the vibrations of an electronic Wigner crystal. *Nat. Phys.* **13**, 340–344 (2017).
38. Liu, Y. et al. Observation of reentrant integer quantum Hall states in the lowest Landau level. *Phys. Rev. Lett.* **109**, 036801 (2012).
39. Liu, Y. et al. Fractional quantum Hall effect and Wigner crystal of interacting composite fermions. *Phys. Rev. Lett.* **113**, 246803 (2014).
40. Kozuka, Y. et al. Insulating phase of a two-dimensional electron gas in $Mg_xZn_{1-x}O$/ZnO heterostructures below $\nu = 1/3$. *Phys. Rev. B* **84**, 033304 (2011).
41. Maryenko, D. et al. Composite fermion liquid to Wigner solid transition in the lowest Landau level of zinc oxide. *Nat. Commun.* **9**, 4356 (2018).
42. Zhou, H., Polshyn, H., Taniguchi, T., Watanabe, K. & Young, A. F. Solids of quantum Hall skyrmions in graphene. *Nat. Phys.* **16**, 154–158 (2020).
43. Villegas Rosales, K. A. et al. Competition between fractional quantum Hall liquid and Wigner solid at small fillings: role of layer thickness and Landau level mixing. *Phys. Rev. Res.* **3**, 013181 (2021).
44. Xia, J. S. et al. Electron correlation in the second Landau level: a competition between many nearly degenerate quantum phases. *Phys. Rev. Lett.* **93**, 176809 (2004).
45. Kumar, A., Csáthy, G. A., Manfra, M. J., Pfeiffer, L. N. & West, K. W. Nonconventional odd-denominator fractional quantum Hall states in the second Landau level. *Phys. Rev. Lett.* **105**, 246808 (2010).
46. Kleinbaum, E., Kumar, A., Pfeiffer, L. N., West, K. W. & Csáthy, G. A. Gap reversal at filling factors 3+1/3 and 3+1/5: towards novel topological order in the fractional quantum Hall regime. *Phys. Rev. Lett.* **114**, 076801 (2015).
47. Koulakov, A. A., Fogler, M. M. & Shklovskii, B. I. Charge density wave in two-dimensional electron liquid in weak magnetic field. *Phys. Rev. Lett.* **76**, 499–502 (1996).
48. Moessner, R. & Chalker, J. T. Exact results for interacting electrons in high Landau levels. *Phys. Rev. B* **54**, 5006–5015 (1996).
49. Lilly, M. P., Cooper, K. B., Eisenstein, J. P., Pfeiffer, L. N. & West, K. W. Evidence for an anisotropic state of two-dimensional electrons in high Landau levels. *Phys. Rev. Lett.* **82**, 394–397 (1999).
50. Du, R. R. et al. Strongly anisotropic transport in higher two-dimensional Landau levels. *Solid State Commun.* **109**, 389–394 (1999).
51. Cooper, K. B., Lilly, M. P., Eisenstein, J. P., Pfeiffer, L. N. & West, K. W. Insulating phases of two-dimensional electrons in high Landau levels: observation of sharp thresholds to conduction. *Phys. Rev. B* **60**, R11285–R11288 (1999).
52. Gervais, G. et al. Competition between a fractional quantum Hall liquid and bubble and Wigner crystal phases in the third Landau level. *Phys. Rev. Lett.* **93**, 266804 (2004).
53. Fu., X. et al. Two- and three-electron bubbles in $Al_xGa_{1-x}As/Al_{0.24}Ga_{0.76}As$ quantum wells. *Phys. Rev. B* **99**, 161402(R) (2019).
54. Ro, D. et al. Electron bubbles and the structure of the orbital wave function. *Phys. Rev. B* **99**, 201111(R) (2019).
55. Yi, H. & Fertig, H. A. Laughlin-Jastrow-correlated Wigner crystal in a strong magnetic field. *Phys. Rev. B* **58**, 4019–4027 (1998).
56. Narevich, R., Murthy, G. & Fertig, H. A. Hamiltonian theory of the composite fermion Wigner crystal. *Phys. Rev. B* **64**, 245326 (2001).
57. Archer, A. C., Park, K. & Jain, J. K. Competing crystal phases in the lowest Landau level. *Phys. Rev. Lett.* **111**, 146804 (2013).
58. Zhao, J., Zhang, Y. & Jain, J. K. Crystallization in the fractional quantum Hall regime induced by Landau-level mixing. *Phys. Rev. Lett.* **121**, 116802 (2018).
59. Deng, N., Watson, J. D., Rokhinson, L. P., Manfra, M. J. & Csáthy, G. A. Contrasting energy scales of reentrant integer quantum Hall states. *Phys. Rev. B* **86**, 201301(R) (2012).

60. Csáthy, G. A. In *Fractional Quantum Hall Effects—New Developments*, (eds Halperin, B. I. & Jain, J. K.) Ch. 5 (World Scientific Publishing Co., 2020).
61. Santos, M. B. et al. Observation of a reentrant insulating phase near the 1/3 fractional quantum Hall liquid in a two-dimensional hole system. *Phys. Rev. Lett.* **68**, 1188–1191 (1992).
62. Li, C.-C., Engel, L. W., Shahar, D., Tsui, D. C. & Shayegan, M. Microwave conductivity resonance of two-dimensional hole system. *Phys. Rev. Lett.* **79**, 1353–1356 (1997).
63. Zhang, C., Du, R. R., Manfra, M. J., Pfeiffer, L. N. & West, K. W. Transport of a sliding Wigner crystal in the four flux composite fermion regime. *Phys. Rev. B* **92**, 075434 (2015).
64. Yang, I., Kang, W., Hannahs, S. T., Pfeiffer, L. N. & West, K. W. Vertical confinement and evolution of reentrant insulating transition in the fractional quantum Hall regime. *Phys. Rev. B* **68**, 121302(R) (2003).
65. Li, W., Luhman, D. R., Tsui, D. C., Pfeiffer, L. N. & West, K. W. Observation of reentrant phases induced by short-range disorder in the lowest Landau level of $Al_xGa_{1-x}As/Al_{0.32}Ga_{0.68}As$ heterostructures. *Phys. Rev. Lett.* **105**, 076803 (2010).
66. Samkharadze, N., Ro, D., Pfeiffer, L. N., West, K. W. & Csáthy, G. A. Observation of an anomalous density-dependent energy gap of the $\nu = 5/2$ fractional quantum Hall state in the low-density regime. *Phys. Rev. B* **96**, 085105 (2017).
67. Chung, Y. J. et al. Ultra-high-quality two-dimensional electron systems. *Nat. Mater.* **20**, 632–637 (2021).
68. Samkharadze, N. et al. Integrated electronic transport and thermometry at milliKelvin temperatures and in strong magnetic fields. *Rev. Sci. Instrum.* **82**, 053902 (2011).
69. Samkharadze, N., Kumar, A. & Csáthy, G. A. A new type of carbon resistance thermometer with excellent thermal contact at millikelvin temperatures. *J. Low. Temp. Phys.* **160**, 246–253 (2010).

Acknowledgements

Measurements at Purdue were supported by the NSF DMR Grant No. 1904497. The sample growth effort of L.N.P. and K.W.B. of Princeton University was supported by the Gordon and Betty Moore Foundation Grant No. GBMF 4420, and the National Science Foundation MRSEC Grant No. DMR-1420541.

Author contributions

V.S. and S.A.M. performed low-temperature transport measurements. L.N.P. and K.W.B. produced MBE-grown GaA/AlGaAs samples and characterized them. V.S., S.A.M. and G.A.C. conceived the project, analyzed the data, and wrote the manuscript.

Competing interests

The authors declare no competing interests.

Additional information

Correspondence and requests for materials should be addressed to GáborA. Csáthy
Peer review information *Communications Physics* thanks Denis Maryenko, Yoshiro Hirayama and the other, anonymous, reviewer(s) for their contribution to the peer review of this work.

Reprints and permission information is available at http://www.nature.com/reprints

Publisher's note Springer Nature remains neutral with regard to jurisdictional claims in published maps and institutional affiliations.